

Supplementary information

Decoration of Metal Oxide Surface with {111} Form Au Nanoparticles Using PEGylation

Cheon Woo Moon, Jongseong Park, Seung-Pyo Hong, Woonbae Sohn, Dinsefa Mensur Andoshe, Mohammadreza Shokouhimehr and Ho Won Jang*

¹ Department of Materials Science and Engineering, Research Institute of Advanced Materials, Seoul National University, Seoul 00826, Republic of Korea.

E-mail: hwjang@snu.ac.kr

Table of contents

1. Supporting Figures S1 ~ S10

1. Supporting Figures

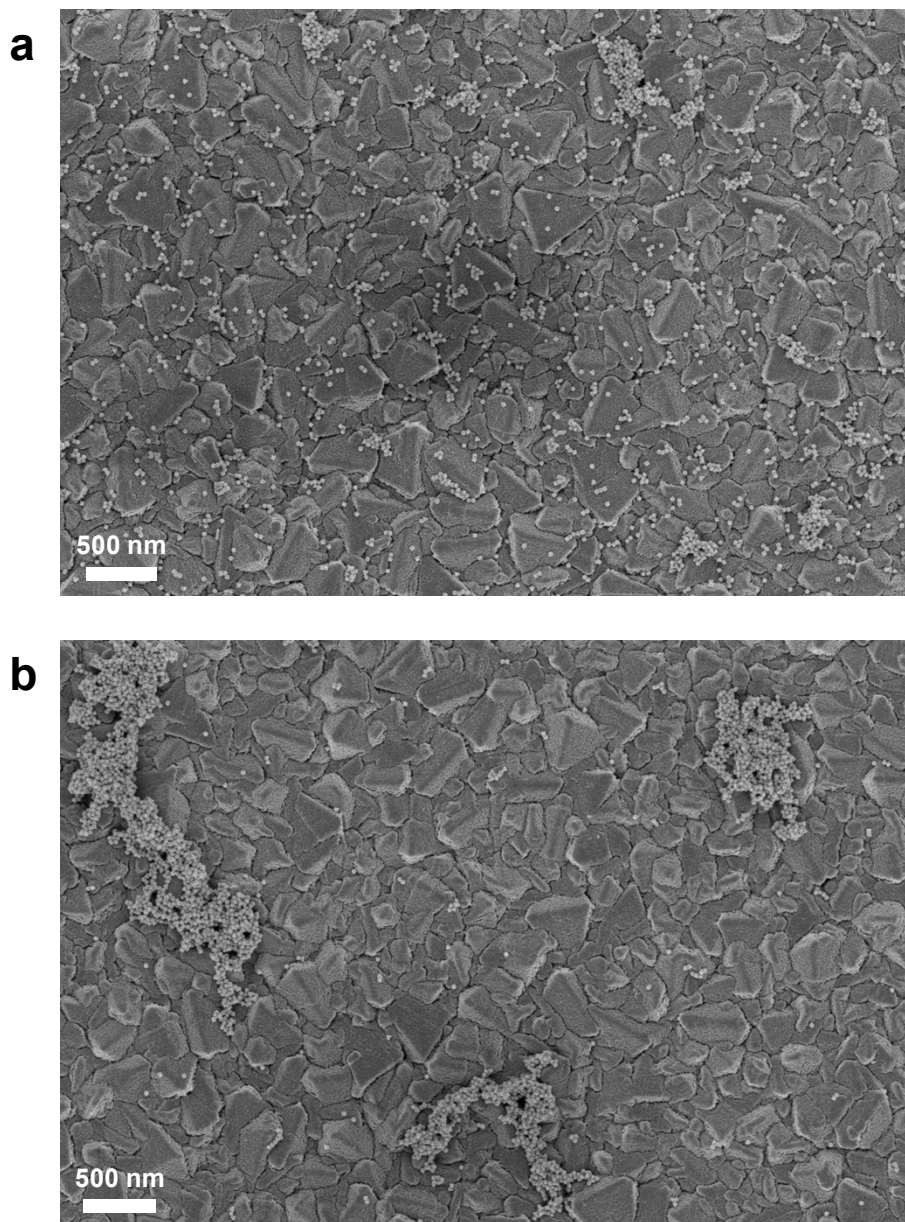


Figure S1. Agglomeration of octahedral Au nanoparticles on TiO₂/FTO on glass substrate. (a) Moderately agglomerated Au nanoparticles (~ 50 %). (b) Heavily agglomerated Au nanoparticles (~ 100 %).

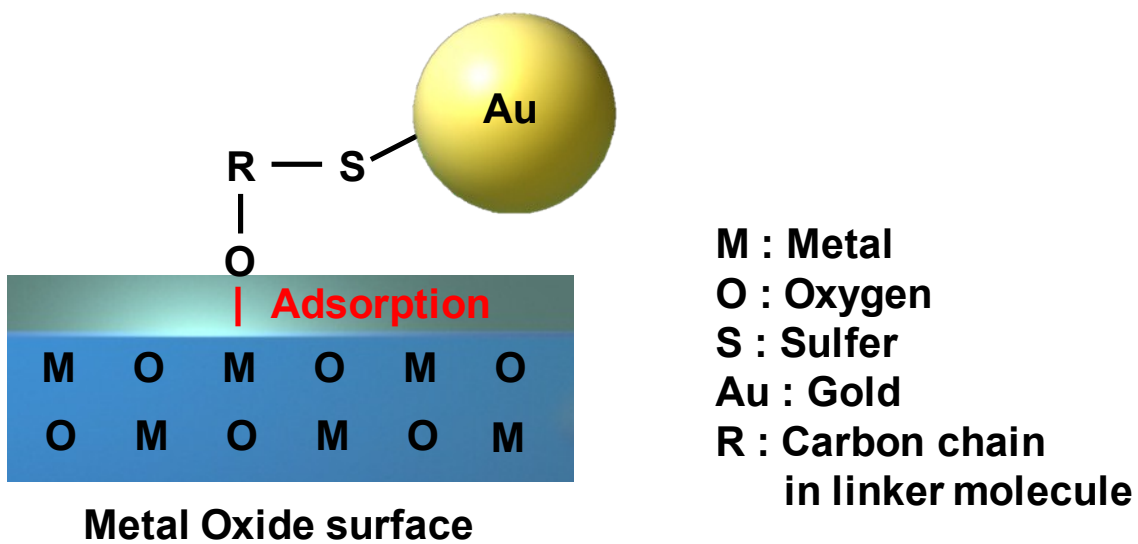
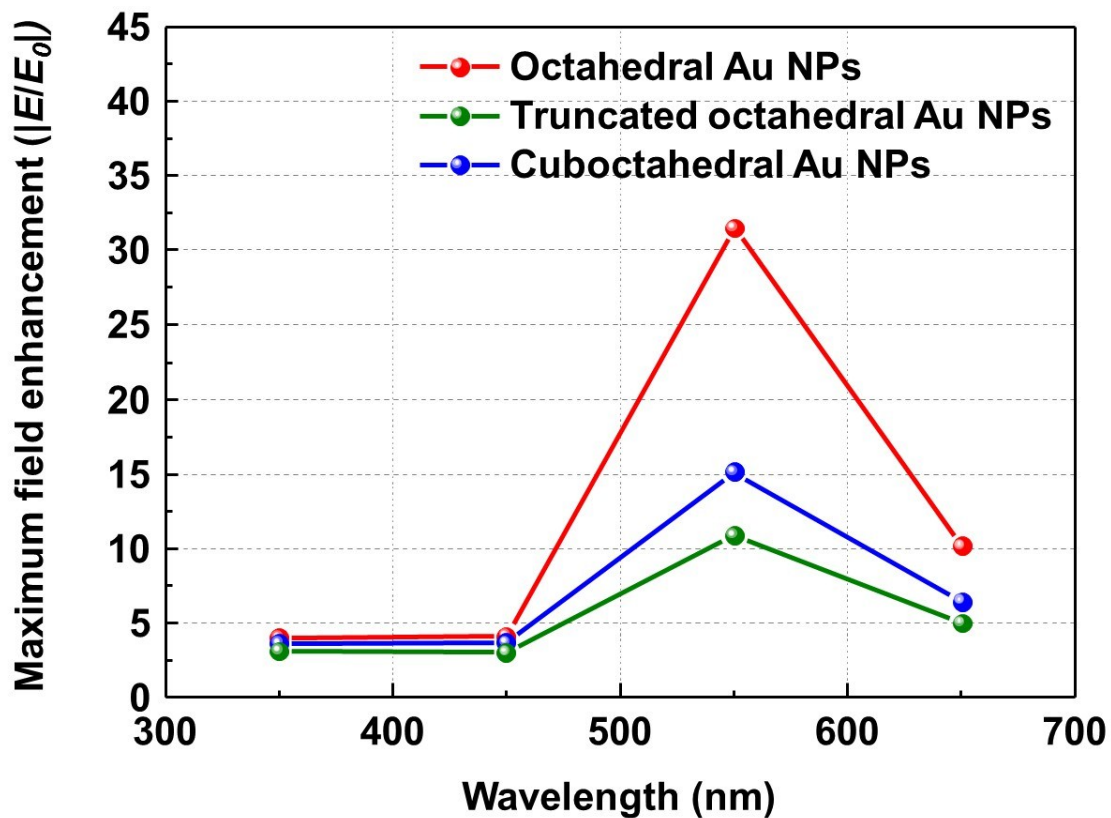

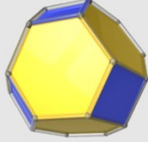
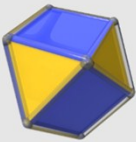


Figure S2. The attachment mechanism of gold nanoparticles using linker molecule from hydroxide (or carboxylic) group.



Wavelength (nm)	350	450	550	650
Octahedral Au NPs	3.995	4.015	31.50	10.135
Truncated octahedral Au NPs	3.107	3.003	10.856	4.978
Cuboctahedral Au NPs	3.62	3.65	15.12	6.43

Figure S3. The maximum electric field enhancement (E/E_0) from twelve finite-difference time-domain (FDTD) simulations. The values are arranged in either graph and table.

	Octahedral Au NPs	Truncated octahedral Au NPs	Cuboctahedral Au NPs
Shape			
(100) portion	0 %	22.4 %	63.4 %
(111) portion	100 %	77.6 %	36.6 %

*Equilateral is assumed.

Figure S4. Calculated coverage of three equilateral shaped Au NPs (octahedral, truncated octahedral and truncated cube) for (100) and (111) facets.

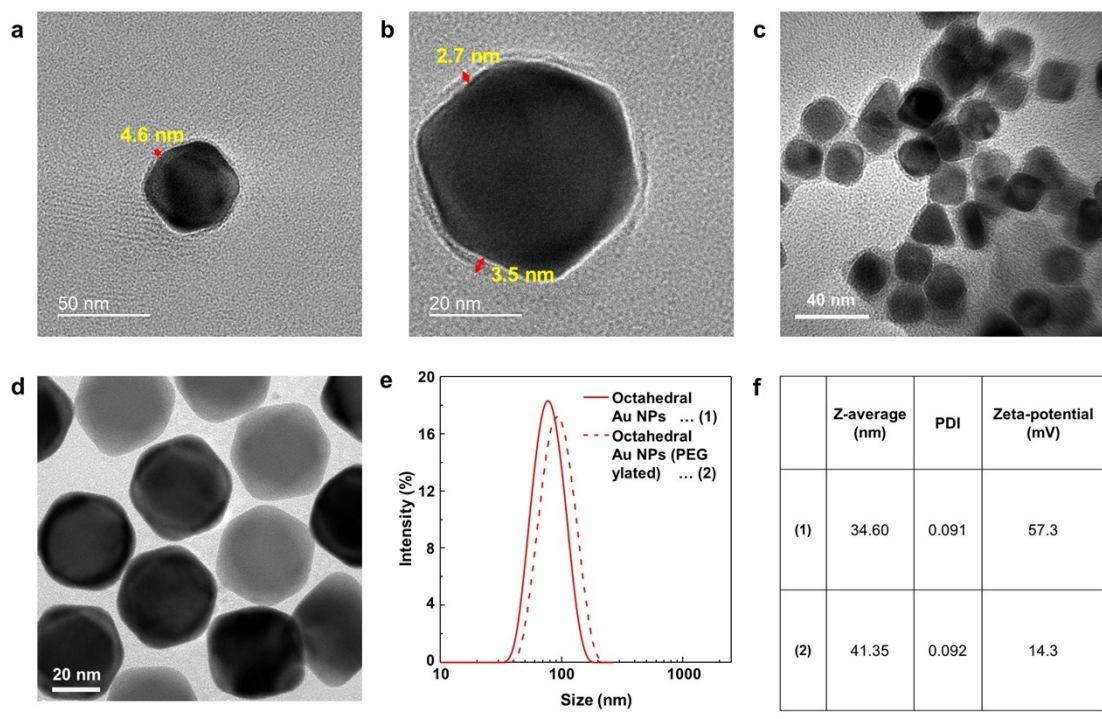


Figure S5. TEM images of PEGylated octahedral Au NPs taken by negative staining technique. (a) Low magnification. (b) High magnification. (c) A bundle of PEGylated octahedral Au NPs on carbon mesh. (d) TEM image of a bundle of pristine octahedral Au NPs on carbon mesh.¹ (e) Dynamic light scattering (DLS) data of Au NPs solutions. The three solutions are denoted as (1), and (2) in the legend. (f) Table for the characteristics of the denoted solutions ((1) and (2)) (polydispersity index; PDI).

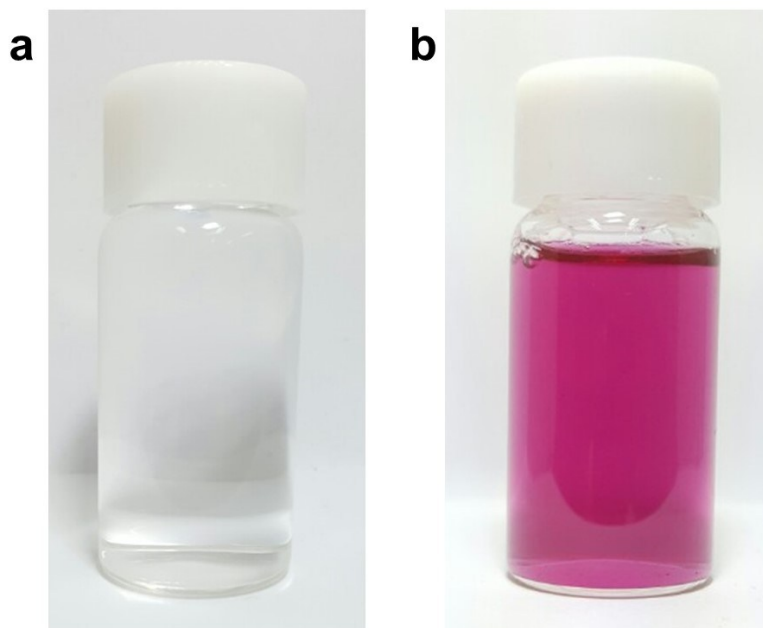


Figure S6. (a) The Au NPs solution (organic phase, EtOH-DCM) after Au octahedral NPs attachment (transparent). (b) The original (aqueous phase) as-synthesized octahedral Au NPs solution (purple).

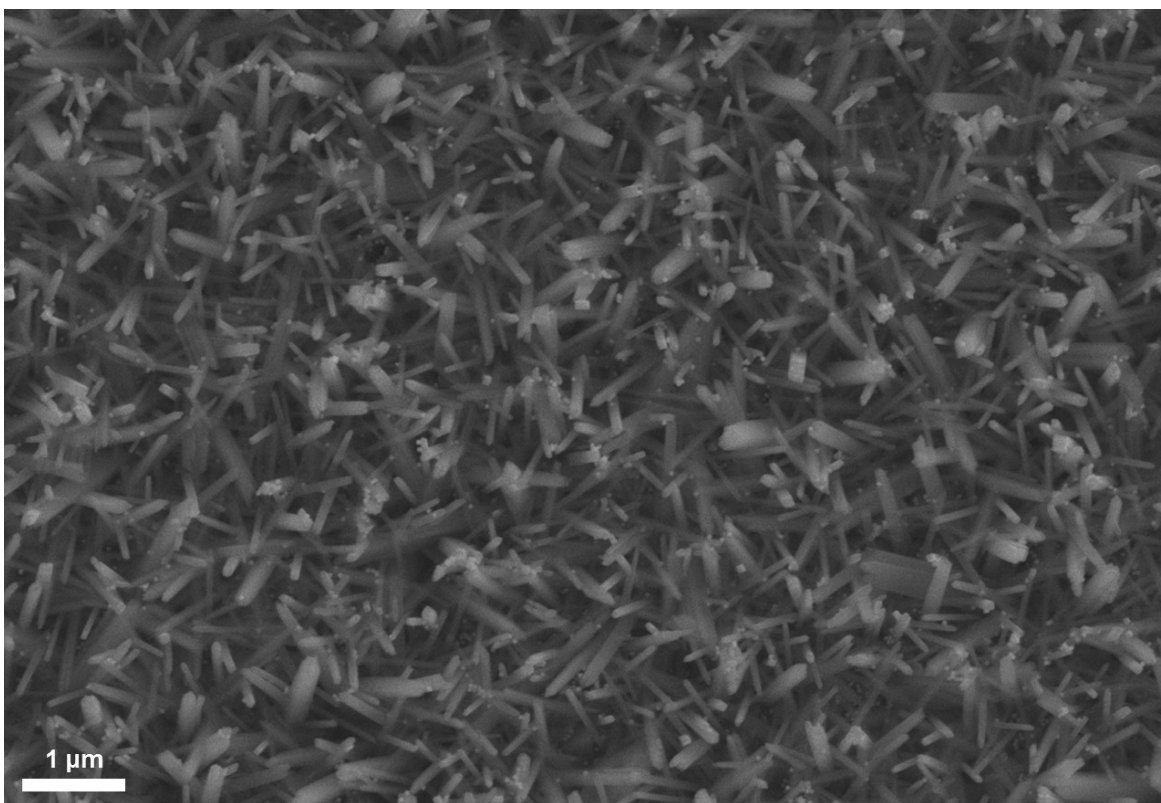


Figure S7. FE-SEM image of octahedral Au NPs decorated TiO₂ nanorods on planar view.

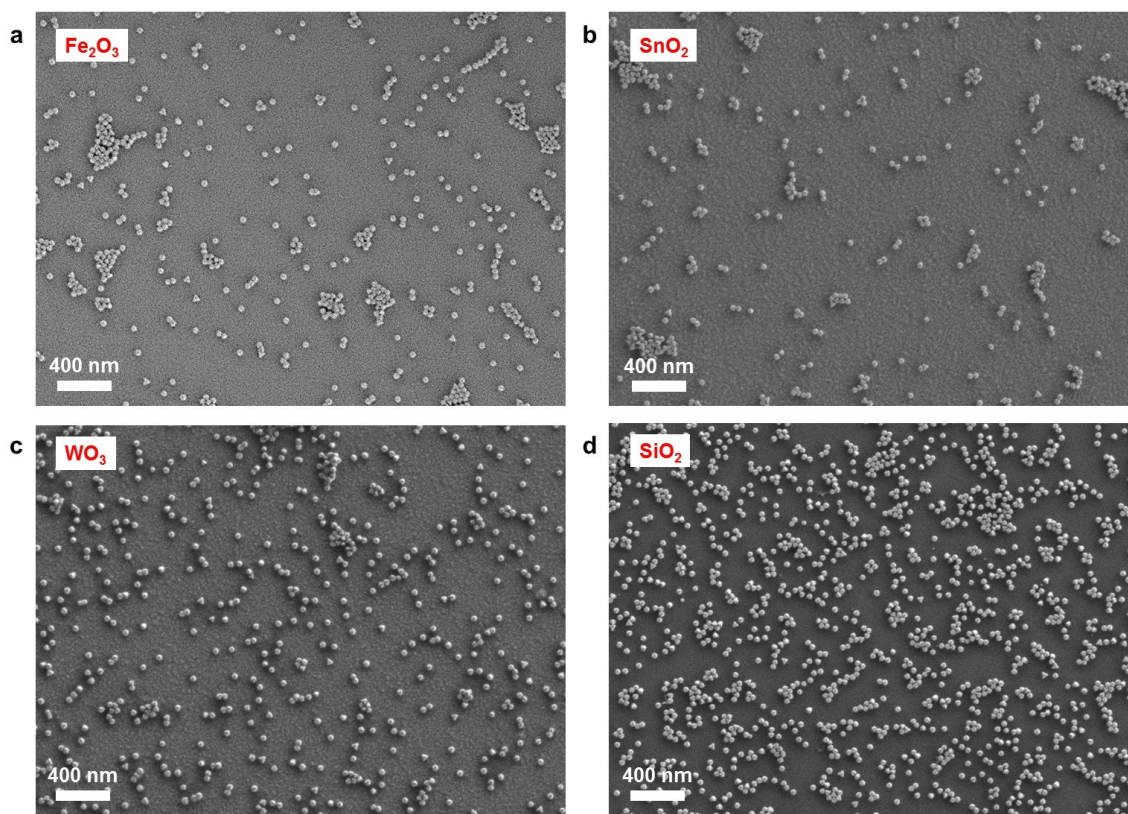
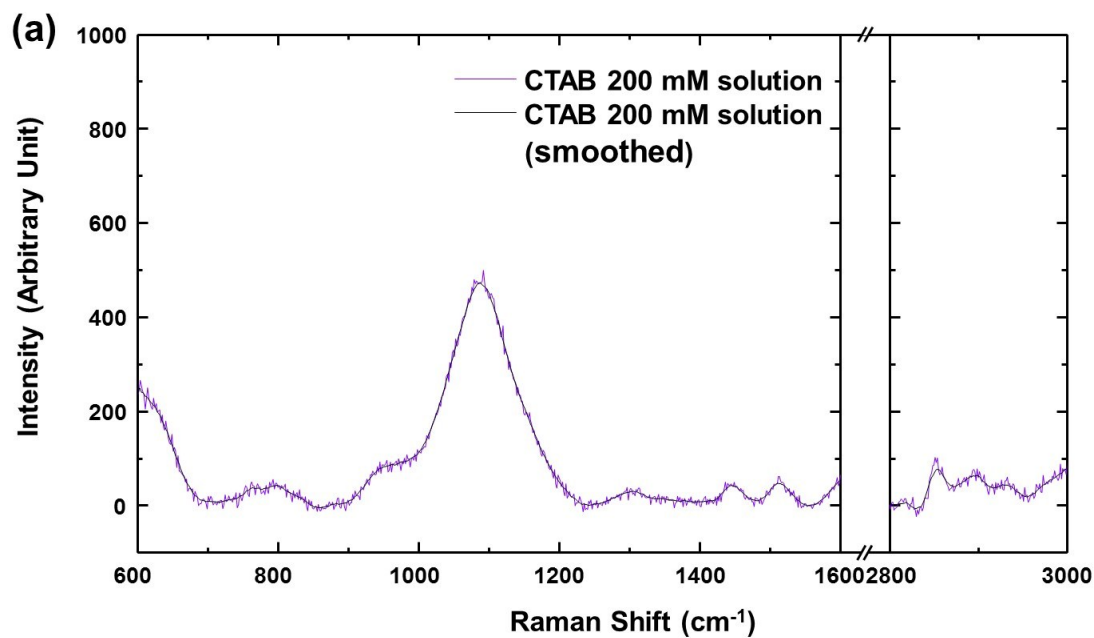


Figure S8. Octahedral Au NPs attachment on various semiconductor. (a) Octahedral Au NPs decorated Fe_2O_3 film (40-nm-thick) on Si substrate. (b) Octahedral Au NPs decorated SnO_2 (40-nm-thick) film on Si substrate. (c) Octahedral Au NPs decorated WO_3 film (40-nm-thick) on Si substrate. (d) Octahedral Au NPs decorated SiO_2/Si substrate.



(b)

Raman peak intensity ratio	Octahedral Au NPs	Truncated octahedral Au NPs	Cuboctahedral Au NPs
$I_{760,PEG} / I_{760}$ (Hydrocarbon chain)	0.602	0.495	0.824
$I_{955,PEG} / I_{955}$ (Headgroup)	0.853	1.05	1.07

Figure S9. (a) Raman spectra of CTAB 200 mM solution. (b) Raman peak intensity ratio before and after PEGylation.

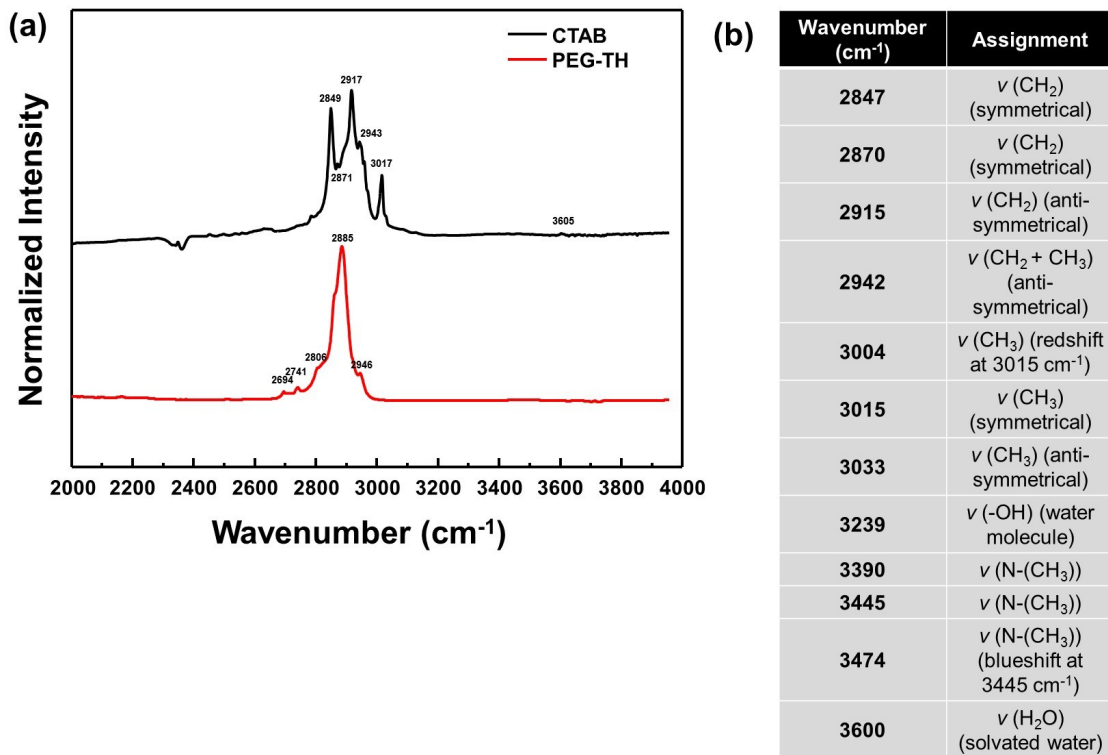


Figure S10. (a) FTIR spectra of the dried CTAB (black) and PEG-TH solution on glass substrate. (b) Peak designation of CTA⁺ molecule in FTIR spectra.

References

1. C. W. Moon, S. Y. Lee, W. Sohn, D. M. Andoshe, D. H. Kim, K. Hong and H. W. Jang, *Part. Part. Sys. Character.*, 2017, 34, 1600340.